ACS APPLIED MATERIALS & INTERFACES

Forum Article

www.acsami.org

Controlled Protein Absorption and Cell Adhesion on Polymer-Brush-Grafted Poly(3,4-ethylenedioxythiophene) Films

Haichao Zhao,*[,†] Bo Zhu,[†] Shyh-Chyang Luo,[†] Hsing-An Lin,[†,‡] Aiko Nakao,[§] Yoshiro Yamashita,[‡] and Hsiao-hua Yu*[,†]

[†]Yu Initiative Research Unit, RIKEN Advanced Science Institute, 2-1 Hirosawa, Wako, Saitama 351-0198, Japan

[‡]Department of Electronic Chemistry, Interdisciplinary Graduate School of Science and Engineering, Tokyo Institute of Technology

[§]RNC Industrial Cooperation Team, RIKEN, Wako, Saitama 351-0198, Japan

Supporting Information

ABSTRACT: Tailoring the surface of biometallic implants with protein-resistant polymer brushes represents an efficient approach to improve the biocompability and mechanical compliance with soft human tissues. A general approach utilizing electropolymerization to form initiating group (-Br) containing poly(3,4-ethylenedioxythiophen)s (poly(EDOT)s) is described. After the conducting polymer is deposited, neutral poly((oligo(ethylene glycol) methacrylate), poly(OEGMA), and zwitterionic poly([2-(methacryloyloxy)ethyl]dimethyl-(3-sulfopropyl)ammonium hydroxide), poly(SBMA), brushes are grafted by surface-initiated atom transfer radical polymerization. Quartz crystal microbalance (QCM) experiments confirm protein resistance of poly(OEGMA) and poly(SBMA)-grafted poly(EDOT)s. The protein binding properties of the surface are modulated by the density of polymer brushes, which is controlled by the feed content of initiator-containing monomer (EDOT-Br) in the monomer mixture solution for electropolymerization. Furthermore, these polymer-grafted poly(EDOT)s also prevent cells to adhere on the surface.

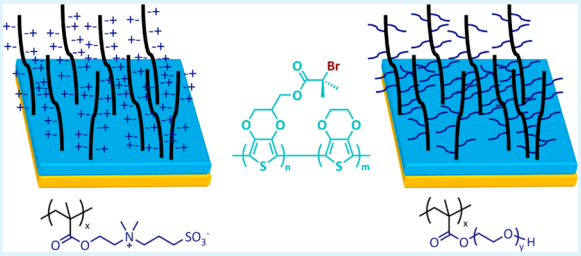

KEYWORDS: *electropolymerization, biomaterial, enzyme resistance, cell adhesion, conducting polymer, polymer brush*

INTRODUCTION

The development of biometallic implants with reduced protein absorption and cell adhesion is critical for many biomedical applications, including biosensors, neural probes, antithrombogenic stents, and prosthetic devices.[1−5] Conventional biometallic implants are based on inert metals such as gold, platinum, iridium oxide, stainless steel, titanium, and titanium alloys. Unfortunately, these materials suffer from low biocompatibility as well as the mismatch of physical, mechanical, and biochemical properties on the device/living-tissue interface. Therefore, tissue inflammations and foreign-object responses are often obserced.[6−15] Moreover, the impedance of these materials inevitably increases because of the adhesion of insulting biolayers composed of nonspecifically bound proteins and cells. As a result, the transduction of electric signals between electronic device and living tissue is reduced with time.[16,17] Until now, the adjustment and matching of mechanical properties, surface properties, bioactivity, and charge transport between the implanted materials and living tissues still remain challenging.[18]

Besides metals, synthetic polymers are increasingly considered for biomedical implants because of their structure flexibility, surface functionality, soft mechanical properties, and controlled biological affinity.[19,20] Among various approaches to utilize polymers for bioimplants, direct modification of a material's surface with enzyme-resistant and soft polymers by surface-initiated polymerization has been proved to be a very convenient approach to improve the biocompatibility and mechanical compliance of hard materials to soft human tissues. At the same time, the durability and robustness of the implants are not sacrificed.[21,22] Among all approaches to utilize synthetic polymers on the surface of metal, atom transfer radical polymerization (ATRP) represents a popular and efficient approach because the polymerization is carried out in a mild condition. Therefore, a wild variety of functional groups are tolerated. It is feasible to create enzyme-resistant polymer grafts from both neutral and zwitterionic polymers,[23] including poly(oligo(ethylene glycol) methacrylate),[24−26] poly(2-methacryloyloxyethyl phosphorylcholine),[27−31] poly(sulfobetaine methacrylate),[32−35] and poly(carboxybetaine methacrylate).[36,37] Surface-initiated ATRP generally include two steps. First, the initiators are grafted onto the surface through covalent linkage. In this step, self-assembled monolayer (SAM) techniques, including thiol-metal bond formation on inert metals and silane-based chemical bond formation on metal oxide surfaces, are typically employed. Subsequently,

Special Issue: Forum on Conjugated Polymer Materials for Sensing and Biomedical Applications

Received: January 11, 2013
Accepted: March 20, 2013
Published: April 10, 2013

   dx.doi.org/10.1021/am400135c | *ACS Appl. Mater. Interfaces* 2013, 5, 4536−4543

ATRP is carried out directly on the surface by immersing the material into the solution containing the catalyst and monomer. Although these SAM-based approaches are often employed, they exhibit certain disadvantageous features. Thiol-metal bonds are usually thermally and electrically unstable, so the shelf life of implants decreases. In the case of silane-based SAM, activation of the metal oxide surface for subsequent chemical transformation usually requires harsh chemical treatment (heat, acid, plasma, etc.) and the formation of uniform silane-based SAM is not easily accomplished.

Electrical conducting polymers (ECPs) such as polyanilines, polypyyroles, and polythiophenes can be electrically deposited onto electrode surfaces with precisely controlled thickness and morphology. Utilizing this method to create initiator-containing thin films on the surface of conductive materials would possibly overcome those disadvantages of SAM-based approaches mentioned earlier. Advincula and co-workers first reported the synthesis and electrodepostion of olefin dendrons with terthiophene moiety.[38] Subsequently, polynorbornene brushes were prepared by surface-initiated ring-opening metathesis polymerization with Grubbs' catalyst. They also demonstrated the combination of eletropolymerization and surface-initiated RAFT (reversible addition−fragmentation chain transfer polymerization) to prepare polymer brushes. In this method, the chain transfer agent was immobilized on the conductive surface by electrodepostion of functionalized terthiophene or carbazole monomers. A variety of polymer brushes were grafted with this surface-initiated RAFT approach.[39−41] More recently, Pei et al. reported a method using electropolymerized poly(pyrrole-*co*-pyrrolyl butyric acid) film on glassy carbon.[42] Initiators were covalently linked to the copolymer film by a two-step process. Zwitterionic polymer brushes were then grafted by surface-initiated ATRP and electrochemical switching properties of these brushes were observed.

Among all ECPs, poly(3,4-ethylenedioxythiophene)s (poly(EDOT)s) represent one of the most promising candidates for biomedical applications. This is due to their low redox potential, high conductivity, and great stability in biological environment. We have recently developed PEDOT-based conductive materials with tunable functionality, controlled nanomorphology, and outstanding cell compatibility.[43−48] Herein, we describe the synthesis of EDOT-based ATRP initiator and it application to graft hydrophilic oligoethylene glycol or sulfobetaine based polymer brushes. We also investigate the controlled protein absorption and cell adhesion on these polymer-brush-grafted poly(EDOT)s.

EXPERIMENTAL SECTION

General Methods. Nuclear magnetic resonance (NMR) spectra were obtained at 25 °C on a Varian 500 spectrometer. Chemical shifts were referenced to residual solvent. Mass spectra were recorded on JMS-700 V (JEOL). X-ray photoelectron spectroscopy (XPS) was performed on an ESCALAB 250 imaging XPS system (Thermo Scientific K.K.). The film surface morphology was examined using atomic force microscopy (NanoScope V, Vecco) with silicon cantilevers (Pointprobe NCH probes, NanoWorld).

Materials. 3,4-ethylenedioxythiophene (EDOT), hydroxymethyl-functionalized EDOT (EDOT−OH), 2-bromoisobutyryl bromide, triethylamine, copper bromide (CuBr), 2,2′-bipyridine, poly(ethylene glycol) methacrylate (OEGMA, M_n = 360), [2-(methacryloyloxy)-ethyl]dimethyl-(3-sulfopropyl)ammonium hydroxide (SBMA), bovine serum albumin (BSA), and fibrinogen were purchased from Sigma-Aldrich. Indium tin oxide (ITO)-coated glass slide was purchased from Delta Technologies, Inc.

Synthesis of 2-Bromo-2-methylpropionic acid-(2,3-dihydrothieno[3,4-b][1,4]dioxin-2-yl)methyl ester (EDOT-Br). To a dry 250 mL three-neck round-bottom flask charged with EDOT−OH (3.4 g, 20 mmol), CH_2Cl_2 (200 mL), triethylamine (3 mL), 2-bromoisobutyryl bromide (4.6 g, 20 mmol) was added slowly via syringe. The solution was allowed to stir overnight. The mixture was then poured into saturated NaCl solution and extracted with ethyl acetate. The organic layer was dried over anhydrous $MgSO_4$, filtered, and the solvent was removed by rotary evaporation under reduced pressure. The crude compound was purified by column chromatography on silica gel (eluent: ethyl acetate/hexane, v/v = 1/2) and dried under a vacuum to yield white powder (5.7 g, 89%). ^{1}H NMR (500 MHz, $CDCl_3$) δ: 1.97 (s, 6H), 4.11 (dd, 1H, J = 12.0, 6.5 Hz), 4.27 (dd, 1H, J = 12.0, 2.0 Hz), 4.38 (dd, 1H, J = 13.0, 7.0 Hz), 4.41−4.46 (m, 2H), 6.35(d, 1H, J = 4 Hz), 6.36 (d, 1H, J = 4 Hz). ^{13}C NMR (125 MHz, $CDCl_3$) δ: 30.6, 55.1, 63.4, 65.4, 71.1, 100.0, 100.1, 141.0, 141.1, 171.2. HR-MS (EI) calculated for $C_{11}H_{13}BrO_4S$ 319.9718 [M +]; found 319.9716.

Preparation of Poly(EDOT-Br) and poly(EDOT-Br-*co*-EDOT) Films by Electropolymerization. Electropolymerization was performed on an Autolab PGSTAT128N potentiostat (Metrohm) using a three-electrode electrochemical cell. A platinum wire electrode was used as the counter electrode and an Ag/$AgNO_3$ electrode (0.01 M of $AgNO_3$ and 0.1 M of Bu_4NPF_6 in CH_3CN) was used as the reference electrode. The total concentration of monomers (pure EDOT-Br or EDOT/EDOT-Br mixture) was constant at 0.01 M in CH3CN containing 0.1 M $LiClO_4$ electrolyte.

Surface-Initiated Atom Transfer Radical Polymerization (ATRP). Polymerization of OEGMA and SBMA were conducted following a similar procefure. Poly(EDOT-Br) or Poly(EDOT-Br-*co*-EDOT) coated conductive substrate, CuBr (43 mg) and 2,2′-bipyridine (220 mg) were added to a 50 mL Schlenk tube and the tube was then sealed. The tube was evacuated and filled with N_2 three times. In another Schlenk tube, poly(ethylene glycol) methacrylate (OEGMA, M_n = 360, 2.0 g) was dissolved in 10 mL methanol/H_2O (v/v = 1/1) and purged with N_2 for 30 min. Afterward, the monomer solution was transferred into the Schlenk tube via a syringe. The polymerization was conducted for 4 h and the substrate was taken out from Schlenk tube, washed with DI water for 3 times, and dried in vacuum for 24 h.

Surface Characterization. X-ray photoelectron spectroscopy (XPS) was conducted by an ESCALAB 250 (Thermo VG) system. The film surface morphology and roughness were examined by atomic force microscopy (NanoScope V, Vecco) with silicon cantilevers (Pointprobe NCH probes, NanoWorld). A sharp edge was created using a razor blade. The thickness was measured by scanning along the cross-section of the edge.

Electrochemical Properties Characterization. The electrochemical impedance spectroscopy (EIS) measurements were performed in PBS buffer in the presence of 10 mM $[Fe(CN)6]^{3-/4-}$ (1:1 mol/mol) as redox couple at 25 °C. The measurement was performed with 10 mV sinusoidal modulation amplitude in the frequency range of 0.1 Hz to 50 kHz at 50 steps upon biasing the working electrode at 0.2 V vs Ag/AgCl.

Protein Absorption. Quartz crystal microbalance (QCM) measurements were performed at 25 °C on a Q-Sense AB system (Biolin Scientific) with a channel flow cell. All the surface modification, including electropolymerization and surface-initiated ATRP, was directly performed on the surface of QSX 301 sensor crystal (Biolin Scientific). The polymer coated QCM crystal was placed in the measurement chamber. A baseline signal was established by allowing PBS buffer to flow at a rate of 20 μL/min until the baseline became stable. Proteins solution (1 mg/mL) of BSA or fibrinogen was flew through the chamber at a flow rate of 20 μL/min. Resonance frequency were measured at 5, 15, 25, 35, 45, 55, and 65 MHz simultaneously. Changes in frequency of the third overtone (n = 3, i.e., 15 MHz) were used for mass analysis.

Cell Adhesion. NIH3T3 fibroblasts were used as the model to evaluate cell attachment. Original ITO coated glass slides (1 cm × 1 cm) used as control experiments. PEDOT films electrodeposited on

these ITO-coated glass slides were used for control experiments as well. Electropolymerization and surface-initiated ATRP were performed under the same reaction condition as previously described. All slides were sterilized by UV light before the cell studies. The slides were placed in tissue culture plate and NIH3T3 fibroblasts were seeded at a density of 2×10^5/mL cells on each sample. Two mL of cellular solution in DMEM buffer with 10% bovine serum was added to the culture plate. The plate was then incubated at 37 °C with 5% CO_2. Attached cells were observed with a phase contrast microscope after 24 h cell culture, respectively.

RESULTS AND DISCUSSION

Preparation of Polymer-Brush-Grafted Poly(3,4-ethylenedioxythiophene)s (PEDOTs). The monomer, EDOT-Br, which could initiate atom transfer radical polymerization (ATRP) was synthesized by esterification of hydroxymethyl functionalized EDOT (EDOT−OH) with 2-bromoisobutyryl bromide in the presence of triethylamine as shown in Scheme 1. The molecular structure of EDOT-Br was confirmed

Scheme 1. Synthesis of the Initiator of Atom Transfer Radical Polymerization (ATRP)

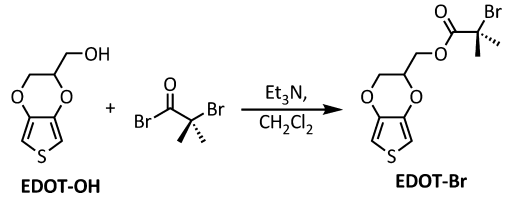

EDOT-OH EDOT-Br

by ^{1}H NMR, ^{13}C NMR, and mass spectroscopy. A two-step procedure was used to form the desired polymer brush-grafted PEDOTs on conductive substrates as illustrated in Scheme 2. First, pure EDOT-Br or EDOT-Br/unfunctionalized-EDOT mixture was electropolymerized directly onto the conductive substrate to form a thin layer of poly(EDOT-Br) or poly(EDOT-Br-*co*-EDOT). Neutral poly(oligo(ethylene glycol) methacrylate), poly(OEGMA), or zwitterionic poly([2-(methacryloyloxy)ethyl]dimethyl-(3-sulfopropyl)ammonium hydroxide), poly(SBMA), brushes were then grafted onto the poly(EDOT) films by ATRP to prepare the desired materials on conductive surfaces.

The electropolymerization step was performed with a standard three-electrode setup in CH_3CN solution containing 10 mM monomer and 0.1 M $LiClO_4$ electrolyte. A cyclic potential from −0.60 to 1.25 V (versus Ag/Ag^+ reference electrode) was applied at a scan rate of 100 mV/s. As shown in Figure 1, continuing increase of cathodic and anodic currents upon each scan indicated the deposition of conductive poly(EDOT-Br) or poly(EDOT-Br-*co*-EDOT) films. Moreover, it was observed visually that blue films were formed on the surface after the first cycle. ATRP was then carried out on initiator containing poly(EDOT-Br) films coated conductive substrates, including gold-coated silicon wafers, gold-coated quartz crystals, and indium tin oxide (ITO) coated glass slides. The substrates were immersed into monomer solution of H_2O/MeOH (50/50 volume ratio) containing CuBr as Cu(I) source and 2,2′-bipyridine as ligand. In general, the electropolymerization step was limited to one cycle of applying potential and ATRP was carried out for 4 h. This was due to the limitation of quartz crystal microbalance (QCM) so we would like to minimize the amount of materials on the surface. After ATRP, the conductive substrates were washed thoroughly with deionized water to remove the catalysts and physically absorbed monomers.

Characterization of PEDOT Films before and after Grafting Polymer Brushes. X-ray photoelectron spectroscopy (XPS) was used to determine the surface composition of electrodeposited poly(EDOT-Br) before and after grafting polymer brushes. The results were summarized in Figure 2. The strong C (1s), O (1s), Br (3d), and S (2p) peaks appeared in Figure 2a indicated the successful deposition of poly(EDOT-Br) on gold surface. In the case of grafted poly(OEGMA) brushes (Figure 2b), we could only observe the reduction of Br peak at 70 eV and the increase of C and O peaks, resulting in a highly reduced Br/C peak ratio. On the other hand, appearance of new N peak (1s) at 402 eV when poly(SBMA) brushes were grafted (Figure 2c) provided more evidences that ATRP was successful.

The surface morphology and thickness of poly(EDOT-Br) films were characterized by atomic force microscope (AFM). As shown in Figure 3a, poly(EDOT-Br) from applying potential for one cycle displayed relative smooth surface (R_{rms} = 5.5 nm). Creation of a sharp edge by blades allowed us to estimate the average thickness of the film as 10.1 nm (see Figure S1 in the Supporting Information). With similar method, we could measure the thickness of poly(OEGMA) and poly(SBMA) brushes. The thickness of poly(OEGMA) brushes was estimated at 147.6 nm and that of poly(SBMA) was estimated at 59.8 nm (Figure 3b, c and Figure S1b, c in the Supporting Information). The surface remained smooth after the polymer brushes were grafted. The root-mean-square roughness (R_{rms}) was measured at 7.5 nm for poly(OEGMA)-grafted poly(EDOT) and 2.8 nm for poly(SBMA)-grafted poly(EDOT).

The surface impedance is also a important feature of conductive biointerface because it indicates the electrical communication between the material and environment. As shown in Figure 4, the surface impedance dropped almost 1 order of magnitude in the low frequency range upon the electrodeposition of poly(EDOT-Br) film. As expected, introduction of nonconductive polymer brushes reduced the surface impedance. However, it was clearly observed that the impedance drop was much smaller in the case of poly(SBMA). This could be attributed to the zwitternoinc nature of poly(SBMA), which lead to higher ionic conductivity. Therefore, the impedance drop was not as dramatic.

Controlled Protein Absorption on Polymer-Brush-Grafted PEDOTs. It is commonly observed that proteins in biological fluids absorb and saturate on materials surface within minutes when the materials are immersed into the fluid. These absorbed proteins further mediate a series of cellular responses. Therefore, the materials lose their original functions. Poly(OEGMA) and poly(SBMA) have been shown to prevent the absorption of proteins. This is the main reason why they are grafted to control the protein binding. We use quartz crystal microbalance (QCM) to monitor in situ protein binding on poly(OEGMA) and poly(SBMA) grafted poly(EDOT)s. Bare and poly(EDOT)-coated gold electrodes were used as control experiments. We chose bovine serum albumin (BSA) and fibrinogen (Fn) as the proteins for absorption studies because BSA is the most abundant protein in the circulatory system and Fn plays an important role in blood clotting and cell adhesion. As shown in Figure 5, dramatic and immediate increases of absorbed proteins (both BSA and Fn) on the crystals were observed in control experiments (bare gold and poly(EDOT) when the proteins were introduced into the solution that flew

Scheme 2. Preparation of Polymer-Brush-Grafted PEDOT Films

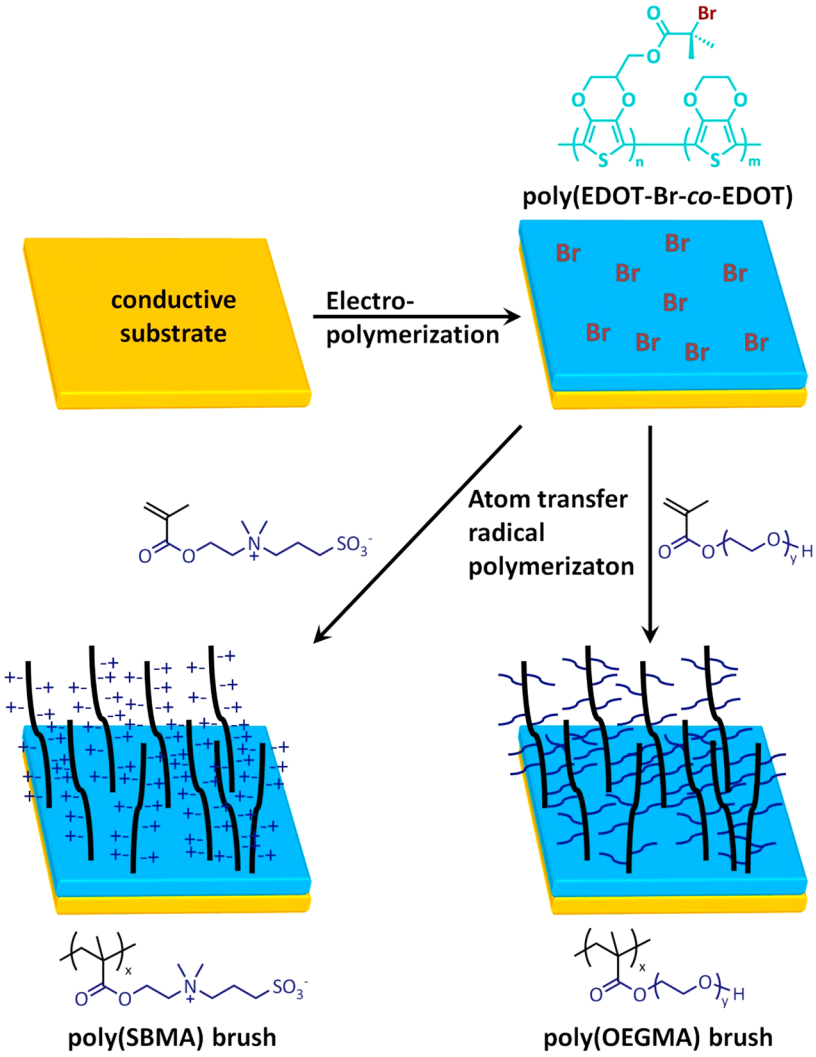

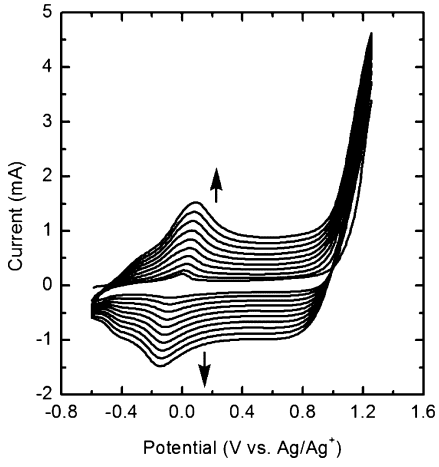

Figure 1. Electropolymerization to form poly(EDOT-Br) films on gold-coated silicon wafers from 10 mM EDOT-Br monomer solution in CH_3CN containing 0.1 M $LiClO_4$ electrolyte. A cyclic potential from −0.60 to 1.25 V is applied.

though the top of the crystals. The protein absorption eventually saturated. Once the fluent switched back to protein-free buffer solution, small mass decreases were observed because loosely bound proteins were washed away. However, majority of the bound proteins remained on the surface. BSA was bound to gold surface at a density of 1046 ng/cm^2 and poly(EDOT) at a density of 529 ng/cm^2. Fn was bound to gold surface at a density of 2750 ng/cm^2 and poly(EDOT) at a density of 1310 ng/cm^2. In contrast, poly(OEGMA) and poly(SBMA) brushes completely inhibited both BSA and Fn binding. The results were in agreement with previous reports on similar polymer brushes grafted by gold−thiol or silane-based approaches.[25,32]

Surface-initiated ATRP allows the fine-tuning of surface properties by controlling the density of grafted polymer brushes. In gold−thiol or silane-based approaches, this was achieved by immobilizing a mixture of molecules which could and could not initiate ATRP.[49,50] In our system, it was expected that the initiator density could be controlled by electropolymerizing a mixture of EDOT-Br and EDOT, which could not initiate ATRP. We measure the composition of poly(EDOT-Br-*co*-EDOT) by XPS (Figure 6) and found that the content of EDOT-Br was lower than the feed composition. The lower EDOT-Br content could be attributed to the slightly higher onset potential when EDOT-Br was oxidized. This phenomenon was observed when pure EDOT-Br was electropolymerized (Figure 1). We applied cyclic potential for

dx.doi.org/10.1021/am400135c | ACS Appl. Mater. Interfaces 2013, 5, 4536−4543

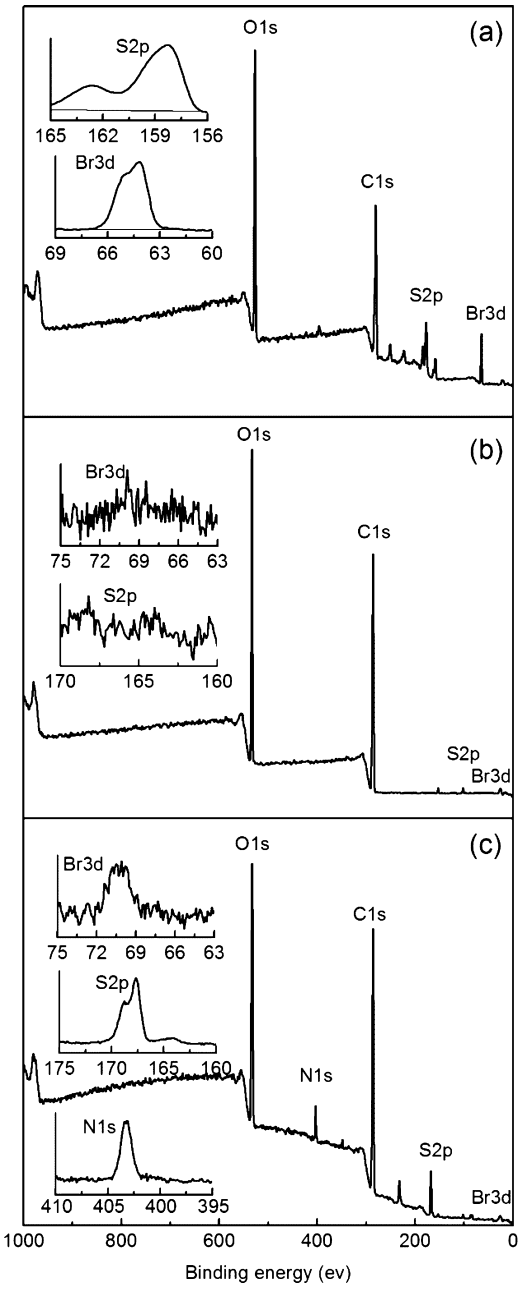

Figure 2. X-ray photoelectron spectra of (a) poly(EDOT-Br), (b) poly(OEGMA)-brush-grafted poly(EDOT), and (c) poly(SBMA)-brush-grafted poly(EDOT).

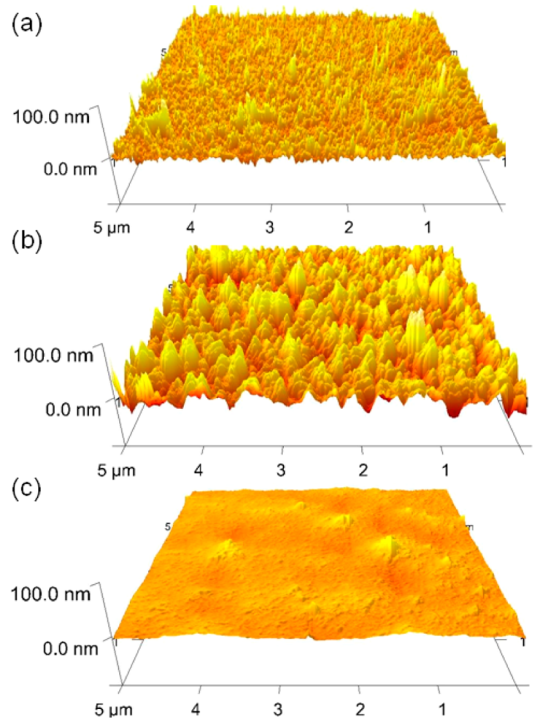

Figure 3. Atomic force microscope (AFM) images of (a) poly(EDOT-Br), (b) poly(OEGMA)-brush-grafted poly(EDOT), and (c) poly(SBMA)-brush-grafted poly(EDOT).

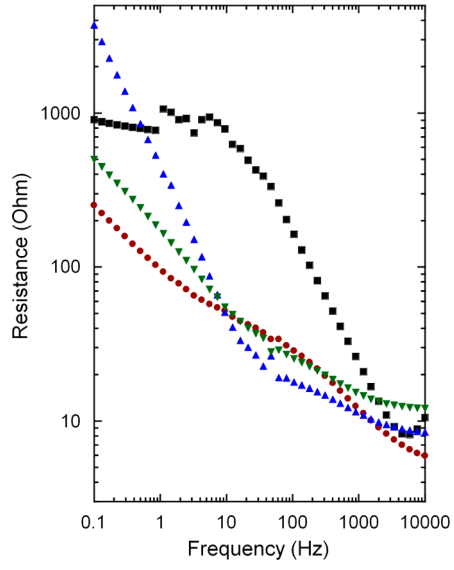

Figure 4. Electrochemical impedance spectroscopy (Bode plots) of gold thin film (■), poly(EDOT-Br) (●), poly(OEGMA)-brush-grafted poly(EDOT) (▲), and poly(SBMA)-brush-grafted poly(EDOT) (▼).

electropolymerization in order to obtain smooth films. Higher onset potential of EDOT-Br could result in lower concentration of reactive EDOT-Br radical near the surface of the electrodes. Therefore, the deposited copolymer films contained lower percentage of EDOT-Br. However, it would be difficult to prove this postulation experimentally. Nevertheless, the measured EDOT-Br content was in linear relationship with the feed EDOT-Br content so the ATRP initiator density still could be modulated by the feed ratio of mixing monomers. As shown in Figure 7, the increase in EDOT-Br content in the monomer mixtures reduced the binding of proteins due to the higher density of enzyme resistant polymer brushes. Even a small incorporation of EDOT-Br (5%) in the monomer mixture could dramatically reduce both BSA and Fn binding by 40%. With the increase in EDOT-Br content in monomer mixture, protein binding decreased. The surface reached the state of enzyme resistance when the feed EDOT-Br composition was greater than 50%. On the basis of our knowledge, this was the first example to utilize electropolymerizaiton in order to control the ATRP initiator density, thereby modulating protein−surface interactions. It could be plausibly applied to control cell adhesion, spreading, and proliferation on conductive metallic substrates.

dx.doi.org/10.1021/am400135c | ACS Appl. Mater. Interfaces 2013, 5, 4536−4543

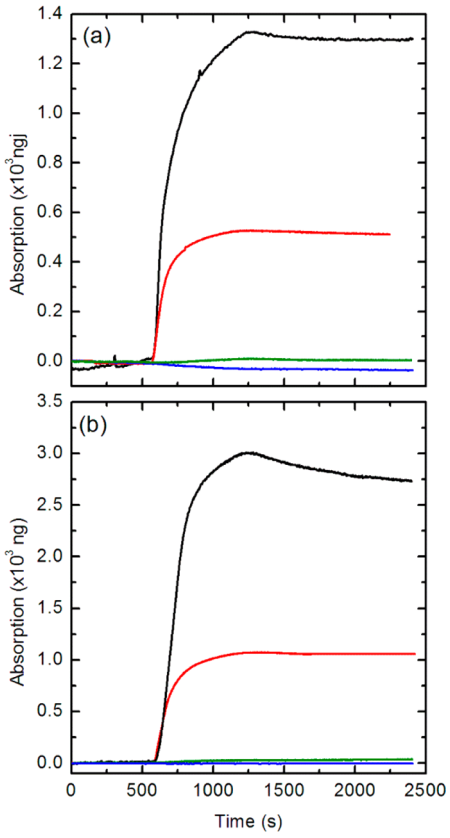

Figure 5. Quartz crystal microbalance (QCM) measurements of (a) bovine serum albumin and (b) fibrinogen absorption on gold (black), poly(EDOT) (red), poly(OEGMA)-brush-grafted poly(EDOT) (blue), and poly(SBMA)-brush-grafted poly(EDOT) (green).

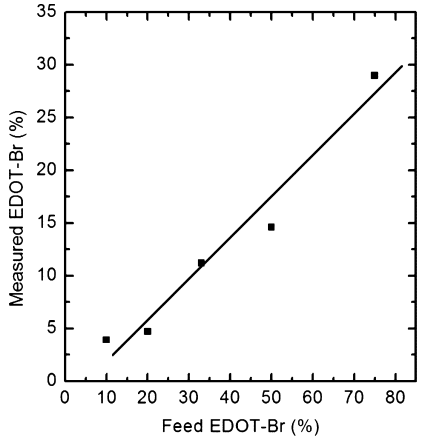

Figure 6. Feed and measured composition of EDOT-Br in poly(EDOT-Br-*co*-EDOT) films electrodeposited from monomer mixtures. The measured composition is determined by X-ray photoelectron spectroscopy (XPS).

Cell adhesion on Polymer-Brush-Grafted PEDOTs. It is well-known that cells do not adhere directly to materials surface. Instead, they bind to proteins in the extracellular matrix (ECM) through integrin receptors. As a result, the surface that can resist protein binding will consequently resist cell adhesion. Using NIH3T3 fibroblast cells, we investigated the cell-binding properties of poly(EDOT) with/without poly(OEGMA) and poly(SBMA) grafts. As show in Figure 8, the cells adhered and spread on bare indium−tin-oxide (ITO)-coated glass slides and

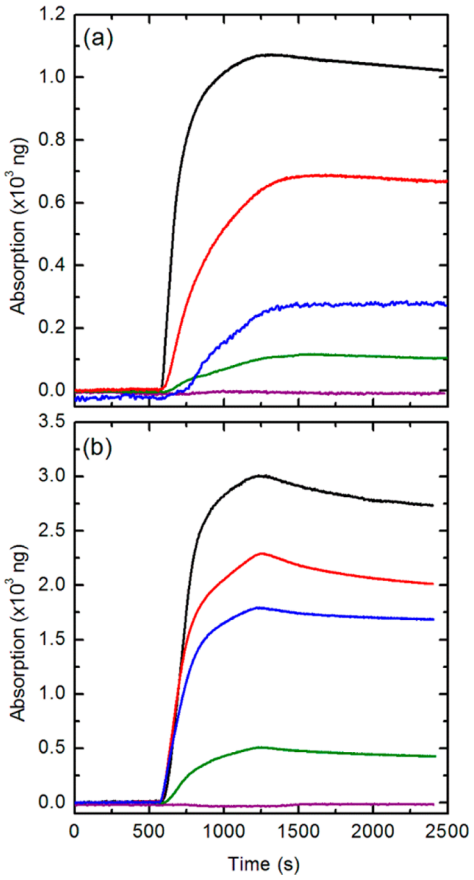

Figure 7. Quartz crystal microbalance (QCM) measurements of (a) bovine serum albumin and (b) fibrinogen absorption on poly(OEGMA)-brush-grafted poly(EDOT) with various densities of polymer brushes. The density of the polymer brush is determined by the monomer composition (EDOT/EDOT-Br) in the mixed monomer solution: 100/0 (black), 95/5 (red), 90/10 (blue), 80/20 (green), and 50/50 (purple).

those slides coated with electropolymerized poly(EDOT). Once poly(OEGMA) and poly(SBMA) brushes were grafted, the films displayed almost no cell adhesion even after 24 h. The results agreed with the conclusions from protein binding experiments. Poly(OEGMA) and poly(SBMA) grafted poly(EDOT) surface could inhibit both protein binding and cell adhesion. Subsequently, the cells could not spread and proliferate.

CONCLUSIONS

We describe herein an approach to fabricate polymer-brush-grafted poly(3,4-ethylenedioxythiophene) films that can be applied for a variety of conductive substrates. First, a mixture of EDOT and a new monomer, EDOT-Br, which is capable of initiating atom transfer radical polymerization (ATRP) electropolymerize directly onto the surface of conductive substrates. Subsequent surface-initiated ATRP is carried out in the presence of Cu(I) catalyst to graft neutral poly((oligo -ethylene glycol) methacrylate), poly(OEGMA), and zwitterionic poly([2-(methacryloyloxy)ethyl]dimethyl-(3-sulfopropyl)-ammonium hydroxide), poly(SBMA), brushes. Results from X-ray photoelectron spectroscopy and atomic force microscope identify the successful formation of polymer brushes onto poly(EDOT). Zwitterionic poly(SBMA) brushes raise the impedance of conductive surface only slightly because of its

dx.doi.org/10.1021/am400135c | *ACS Appl. Mater. Interfaces* 2013, 5, 4536−4543

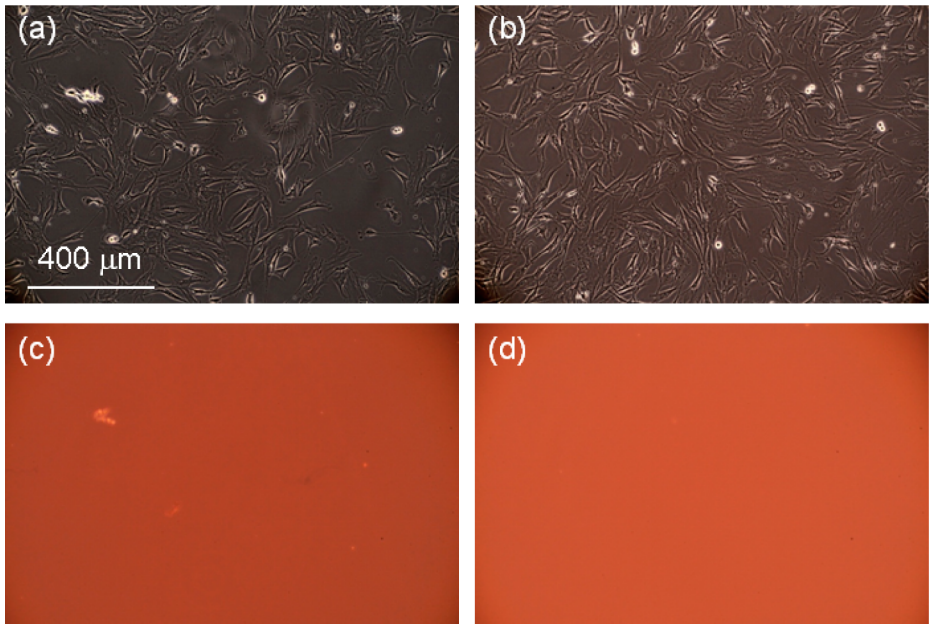

Figure 8. Microscope images of NIH3T3 fibroblasts attached on (a) indium tin oxide (ITO)-coated glass slide, (b) poly(EDOT), which is deposited on ITO-coated glass slide, (c) poly(OEGMA)-brush-grafted poly(EDOT), and (d) poly(SBMA)-brush-grafted poly(EDOT) after incubation for 24 h.

high ionic conductivity. On the other hand, a dramatic increase in surface impedance is observed upon the grafting of neutral poly(OEGMA). Quartz crystal microbalance (QCM) experiments confirms protein resistance of poly(OEGMA) and poly(SBMA) grafted poly(EDOT)s. The protein binding properties of the surface can be modulated by the density of polymer brushes, which is controlled by the feed content of EDOT-Br in the monomer mixture solution during electropolymerization. Because of the enzyme resistance, these polymer-brush-grafted poly(EDOT)s also prevent cell adhesion. Our approach on controlling the enzyme absorption and cell adhesion with polymer-brush-grafted poly(EDOT) shows potentials for biometallic implant applications.

■ ASSOCIATED CONTENT

Supporting Information

Height images from atomic force microscope measurements of poly(EDOT-Br)-, poly(OEGMA)-, and poly(SBMA)-brush-grafted poly(EDOT)s. This material is available free of charge via the Internet at http://pubs.acs.org.

■ AUTHOR INFORMATION

Corresponding Author

*E-mail: haichaozhao@riken.jp, bruceyu@riken.jp.

Notes

The authors declare no competing financial interest.

■ ACKNOWLEDGMENTS

This work was supported by RIKEN Advanced Science Institute and Grant-in-Aid for Young Scientist (22681016 and 23700565) from JSPS/MEXT, Japan. B.Z. thanks RIKEN for a Special Postdoctoral Researcher Fellowship.

■ REFERENCES

(1) Horbett, T. A.; Ratner, B. D.; Schakenraad, J. M.; Schoen, F. J. *Part II Biology, Biochemistry, and Medicine in Biomaterials Science: An Introduction to Materials in Medicine*; Ratner, B. D., Hoffmann, A. S., Schoen, F. J., Lemons, J. E., Eds.; Academic Press: San Diego, CA, pp 133−165.
(2) Eshet, I.; Freger, V.; Kasher, R.; Herzberg, M.; Lei, J.; Ulbricht, M. *Biomacromolecules* **2011**, *12*, 2681−2685.
(3) Bajpai, A. K. *J. Mater. Sci.−Mater. Med.* **2008**, *19*, 343−357.
(4) Banerjee, I.; Pangule, R. C.; Kane, R. S. *Adv. Mater.* **2011**, *23*, 690−718.
(5) Rusmini, F.; Zhong, Z.; Feijen, J. *Biomacromolecules* **2007**, *8*, 1775−1789.
(6) Martin, D. C. *Microsc. Microanal.* **2010**, *16*, 1022−1023.
(7) Lu, Y.; Wang, D.; Li, T.; Zhao, X.; Cao, Y.; Yang, H.; Duan, Y. Y. *Biomaterials* **2009**, *30*, 4143−4151.
(8) Zhong, Y.; Yu, X.; Gilbert, R.; Ravi, B.; Bellamkonda, R. V. *J. Rehabil. Res. Dev.* **2001**, *38*, 627−623.
(9) Abidian, M. R.; Martin, D. C. *Biomaterials* **2008**, *29*, 1273−1283.
(10) Kim, T. G.; Lee, H.; Jang, Y.; Park, T. G. *Biomacromolecules* **2009**, *10*, 1532−1539.
(11) Fan, X.; Lin, L.; Messersmith, P. B. *Biomacromolecules* **2006**, *7*, 2443−2448.
(12) Khoo, X.; Hamilton, P.; O'Toole, G. A.; Snyder, B. D.; Kenan, D. J.; Grinstaff, M. W. *J. Am. Chem. Soc.* **2009**, *131*, 10992−10997.
(13) Malisova, B.; Tosatti, S.; Textro, M.; Gademann, K.; Züurcher, S. *Langmuir* **2010**, *26*, 4018−4026.
(14) Gillich, T.; Benetti, E. M.; Rakhmatullina, E.; Konradi, R.; Li, W.; Zhang, A.; Schlüter, A. D.; Textor, M. *J. Am. Chem. Soc.* **2011**, *133*, 10940−10950.
(15) Li, Y.; Giesbers, G.; Gerth, M.; Zuihof, H. *Langmuir* **2012**, *28*, 12509−12517.
(16) Wallace, G. G.; Moulton, S. E.; Clark, G. M. *Science* **2009**, *324*, 185−186.
(17) Butson, C. R.; Maks, C. B.; McIntyre, C. C. *Clin. Neurophysiol.* **2006**, *117*, 447−454.
(18) Shingo, T.; Nakashima, H.; Torimitsu, K. *PloS One* **2012**, *7*, e33689.
(19) Nair, L. S.; Laurencin, C. T. *Adv. Biochem. Eng./Biotechnol.* **2006**, *102*, 47−90.
(20) Kohane, D.; Langer, R. *Pediatr. Res.* **2008**, *63*, 487−491.
(21) Meyers, S. R.; Grinstaff, M. W. *Chem. Rev.* **2012**, *112*, 1615−1632.
(22) Barbey, R.; Lavanant, L.; Paripovic, D.; Schüwer, N.; Sugnaux, C.; Tugulu, S.; Klok, H. *Chem. Rev.* **2009**, *109*, 5437−5527.

(23) Matyjaszewski, K.; Tsarevsky, N. V. *Chem. Rev.* **2007**, *107*, 2270−2299.
(24) Ma, H.; Hyun, J.; Stiller, P.; Chilkoti, A. *Adv. Mater.* **2004**, *16*, 338−341.
(25) Hucknall, A.; Rangarajan, S.; Chilkoti, A. *Adv. Mater.* **2009**, *21*, 2441−2446.
(26) Ma, H.; Li, D.; Sheng, X.; Zhao, B.; Chilkoti, A. *Langmuir* **2006**, *22*, 3751−3756. Tugulu, S.; Klok, H. *Biomacromolecules* **2008**, *9*, 906−912.
(27) Monge, S.; Canniccioni, B.; Graillot, A.; Bobin, J. *Biomacromolecules* **2011**, *12*, 1973−1982.
(28) Kobayashi, M.; Terayama, Y.; Yamaguchi, H.; Terada, M.; Murakami, D.; Ishihara, K.; Takahara, A. *Langmuir* **2012**, *28*, 7212−7222.
(29) Nishizawa, K.; Konno, T.; Takai, M.; Ishihara, K. *Biomacromolecules* **2008**, *9*, 403−407.
(30) Xu, Y.; Takai, M.; Ishihara, K. *Biomacromolecules* **2009**, *10*, 267−274.
(31) Yoshimoto, K.; Hirase, T.; Madsen, J.; Armes, S. P.; Nagasaki, Y. *Macromol. Rapid Commun.* **2009**, *30*, 2136−40.
(32) Zhang, Z.; Chen, S.; Chang, Y.; Jiang, S. *J. Phys. Chem. B* **2006**, *110*, 10799−10804.
(33) Chang, Y.; Chang, W.; Shih, Y.; Wei, T.; Hsiue, G. *ACS Appl. Mater. Interfaces* **2011**, *3*, 1228−1237.
(34) Chang, Y.; Liao, S.; Higuchi, A.; Ruaan, R.; Chu, C.; Chen, W. *Langmuir* **2008**, *24*, 5453−5458.
(35) Kuo, W.; Wang, M.; Chien, H.; Wei, T.; Lee, C.; Tsai, W. *Biomacromolecules* **2011**, *12*, 4348−4356.
(36) Zhang, Z.; Chen, S.; Jiang, S. *Biomacromolecules* **2006**, *7*, 3311−3315.
(37) Yang, W.; Xue, H.; Li, W.; Zhang, J.; Jiang, S. *Langmuir* **2009**, *25*, 11911−11916.
(38) Jiang, G.; Ponnapati, R.; Pernites, R.; Felipe, M. J.; Advincula, R. *Macromolecules* **2010**, *43*, 10262−10274.
(39) Grande, C. D.; Tria, M. C.; Jiang, G.; Ponnapati, R.; Advincula, R. *Macromolecules* **2011**, *44*, 966−975.
(40) Pernites, R. B.; Foster, E. L.; Felipe, M. J.; Robinson, M.; Advincula, R. *Adv. Mater.* **2011**, *23*, 1287−1292.
(41) Tria, M. C. R.; Grande, C. D. T.; Ponnapati, R. R.; Advincula, R. C. *Biomacromolecules* **2010**, *11*, 3422−3431.
(42) Pei, Y.; Travas-Sejdic, J.; Williams, D. E. *Langmuir* **2012**, *28*, 8072−8083.
(43) Luo, S.; Ali, E. M.; Tansil, N. C.; Yu, H.; Gao, S.; Kantchev, E. A. B.; Ying, J. Y. *Langmuir* **2008**, *24*, 8071−8077.
(44) Luo, S.; Sekine, J.; Zhu, B.; Zhao, H.; Nakao, A.; Yu, H. *ACS Nano* **2012**, *6*, 3018−3026.
(45) Zhao, H.; Zhu, B.; Sekine, J.; Luo, S.-C.; Yu, H.-h. *ACS Appl. Mater. Interfaces* **2012**, *4*, 680−686.
(46) Sekine, J.; Luo, S.-C.; Wang, S.; Zhu, B.; Tseng, H. R.; Yu, H.-h. *Adv. Mater.* **2011**, *23*, 4788−4792.
(47) Luo, S.-C.; Zhu, B.; Kantchev, E. A. B.; Siang, Y. W.; Yu, H.-h. *Chem. Commun.* **2012**, *48*, 6942−6944.
(48) Luo, S.-C.; Zhu, B.; Nakao, A.; Nakatomi, R.; Yu, H.-h. *Adv. Eng. Mater.* **2011**, *13*, B423−B427.
(49) Ma, H.; He, J.; Liu, X.; Gan, J.; Jin, G.; Zhou, J. *ACS Appl. Mater. Interfaces* **2010**, *2*, 3223−3230.
(50) Brown, A. A.; Khan, N. S.; Steinbock, L.; Huck, W. T. S. *Eur. Polym. J.* **2005**, *41*, 1757−1765.